1   **An Innovative Photoreactor, FluHelik, To Promote UVC/H₂O₂**

2   **Photochemical Reactions: Tertiary Treatment of an Urban**

3   **Wastewater**

4   Jonathan C. Espíndola[1,2], Raquel O. Cristóvão[1,*], Sara R.F. Araújo[1], Teresa Neuparth[3],

5   Miguel M. Santos[3,4], Rosa Montes[5], José B. Quintana[5], Rosario Rodil[5], Rui A.R.

6   Boaventura[1], Vítor J. P. Vilar[1,*]

7

8   *[1]Laboratory of Separation and Reaction Engineering - Laboratory of Catalysis and Materials*

9   *(LSRE-LCM), Department of Chemical Engineering, Faculty of Engineering, University of*

10 *Porto, Rua Dr. Roberto Frias, 4200-465, Porto, Portugal*

11 *[2]CNPq - National Council for Scientific and Technological Development, Brazil*

12 *[3]CIMAR/CIIMAR - LA, Interdisciplinary Centre of Marine and Environmental Research,*

13 *Avenida General Norton de Matos S/N, 4450-208 Matosinhos, Portugal*

14 *[4]FCUP – Department of Biology, Faculty of Sciences, University of Porto, Rua do Campo*

15 *Alegre, 4169-007 Porto, Portugal.*

16 *[5]Department of Analytical Chemistry, Nutrition and Food Sciences, IIAA—Institute for Food*

17 *Analysis and Research, Universidade de Santiago de Compostela, Constantino Candeira S/N,*

18 *15782 Santiago de Compostela, Spain*
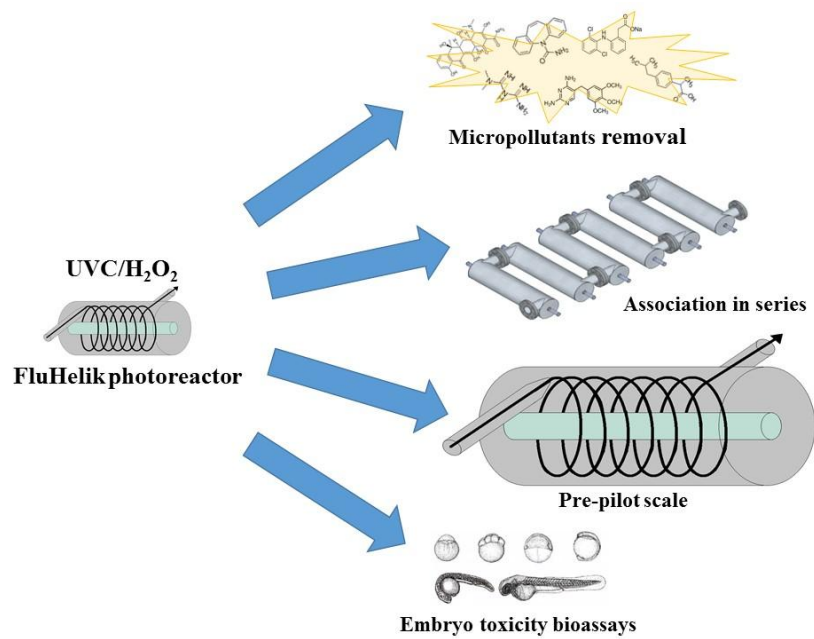
19

20

21 *Corresponding authors:

22 R.O. Cristóvão:

23 *Tel:* +351 22 041 3606; *E-mail*: raquel.cristovao@fe.up.pt

24 Vítor J. P. Vilar:

25 *Tel:* +351 91 825 7824; *E-mail:* vilar@fe.up.pt

26 Fax: +351 22 508 1674

Graphical Abstract

UVC/H$_2$O$_2$

FluHelik photoreactor

Micropollutants removal

Association in series

Pre-pilot scale

Embryo toxicity bioassays

Highlights

- The FluHelik photoreactor proved to enhance the OTC oxidation by UVC/H_2O_2;

- The FluHelik design showed superior performance than conventional Jets photoreactor;

- FluHelik reactor + UVC/H_2O_2 effectively reduced CECs complying with Swiss legislation;

- FluHelik reactor + UVC/H_2O_2 effectively reduced CECs toxicity to zebrafish embryos;

- The FluHelik scale-up proved to be feasible employing several reactors in series.

Abstract

An innovative photoreactor, FluHelik, was used to promote the degradation of contaminants of emerging concern (CECs) by a photochemical UVC/H_2O_2 process. First, the system was optimized for the oxidation of a model antibiotic, oxytetracycline (OTC), using both ultrapure water (UPW) and a real urban wastewater (UWW) (collected after secondary treatment) as solution matrices. Following, the process was evaluated for the treatment of a UWW spiked with a mixture of OTC and 10 different pharmaceuticals established by the Swiss legislation at residual concentrations ($\sum$CECs < 660 μg L^{-1}). The performance of the FluHelik reactor was analyzed both at lab and pre-pilot scale in multiple and single pass flow modes.

The efficiency of the FluHelik photoreactor, at lab-scale, was evaluated at different operational conditions (H_2O_2 concentration, UVC lamp power (4, 6 and 11 W) and flow rate) and further compared with a conventional Jets photoreactor. Both photoreactors exhibited similar OTC removal efficiencies at the best conditions; however, the FluHelik reactor showed to be more efficient (1.3 times) in terms of mineralization when compared with the Jets reactor. Additionally, the efficiency of the UVC/H_2O_2 photochemical system using the FluHelik photoreactor in reducing the toxicity of the real effluent containing 11 pharmaceuticals was evaluated through zebrafish (*Danio rerio*) embryo toxicity bioassays. FluHelik scale-up from laboratory to pre-pilot to promote UVC/H_2O_2 photochemical process proved to be feasible.

Keywords: FluHelik photoreactor; UVC/H_2O_2; CECs; Urban wastewater; Zebrafish embryo toxicity test.

Introduction

UVC/H_2O_2 photochemical process is based in the homolytic cleavage of H_2O_2 molecules by UVC light, resulting in highly reactive species (HO$^\bullet$), able to eliminate an extensive variety of pollutants from water. However, due to the low values of molar absorption coefficient of H_2O_2 at 254 nm, high H_2O_2 or UV dose is required to achieve an efficient performance (Krishnan et al., 2017). On the other hand, urban wastewaters composition can reduce significantly the system efficiency due to the presence of light absorbing species (NOM, nitrite, etc.) (Diya'uddeen et al., 2011). The efficiency of UVC/H_2O_2 photochemical process is also largely influenced by the reactor hydrodynamics regime, which must promote an uniform UV fluence within the reactor (Cambié et al., 2016). Here enters the importance of the reaction mixing conditions for the treatment effectiveness (Karpel VelLeitner et al., 1997). Several commercial reactors incorporate different mixing systems, such as static mixers and conical dispersion components, to improve the degree of mixing inside the reactor, promoting the contact between reagents/pollutants and the emitted UVC photons. Normally, the irradiation source is located in the most turbulent zone of the reactor (Masschelein, 1992). Nowadays there is a great variety of photoreactors with diverse geometries leading to different hydrodynamics. Generally, the photoreactor comprises a cylindrical shell of stainless steel housing a concentric quartz sleeve filled with an UVC lamp and the water to be treated flows between the concentric tubes (annular reactor). However, the irradiation source may be also external, such as the parallel plate reactors or cylindrical reactors reported by Noël (2017)). The mixing and irradiation conditions can also be improved through introduction of a multi-lamp design (Boyjoo et al., 2014) or by usage of rotating annular reactors (Subramanian and Kannan, 2010) or spinning disc reactors (Yatmaz et al., 2001). Therefore, even with the same lamp type and intensity,

75 reagents/pollutants dosages and similar flow rates, the photons dissemination as well

76 and the pollutants removal may be completely different (Caris, 2011). Although

77 photochemical reactors have been already applied in water/wastewater treatment plants,

78 the process is not widely disseminated because of the inherent limitations that it

79 presents, namely in terms of energy costs and efficiency. Therefore, breakthrough

80 designs for photoreactors are required to achieve a cost-effective treatment solution (Su

81 et al., 2014).

82 The present work focuses on the application of an innovative photoreactor, FluHelik, in

83 the removal of contaminants of emerging concern (CECs) from urban wastewaters, as a

84 polishing step, using a UVC/H_2O_2 photochemical process. The FluHelik photoreator

85 comprises a cylindrical shell of stainless steel, internally polished, with inlet and outlet

86 pipes located perpendicularly to the fluid flow and tangentially to the shell in horizontal

87 plane and at the top in opposite sides. A concentric inner quartz sleeve houses an UVC

88 lamp. This configuration induces unique fluid dynamics (high degree of mixing) and

89 irradiation properties (a more homogeneous UV radiation distribution) by promoting a

90 helical motion of the fluid around the UVC lamp. First, synthetic solutions of OTC or

91 UWW fortified with OTC were used as reaction matrices. Two configurations of

92 photoreactors were employed: FluHelik and Jets (four inlet and four outlet pipes placed

93 in parallel with the fluid flow direction at the ends of the tube). Process efficiency was

94 evaluated as a function of several operational conditions, namely: (i) recirculation flow

95 rate, (ii) H_2O_2 concentration and (iii) UVC lamp power. In addition, the feasibility of

96 implementing the FluHelik reactor for the UVC/H_2O_2 process was tested both at

97 laboratory and at pre-pilot scale either in multiple or single pass flow mode. Finally, the

98 treatment of a real urban wastewater matrix spiked with a mixture of 11 CECs, at

99 residual concentrations, was evaluated using the FluHelik photoreactor and the

100 UVC/H_2O_2 system.

101 Considering that oxidation by-products might be more toxic and/or persistent than the

102 parent compounds, toxicological studies are needed to determine their deleterious

103 effects on ecosystems and human health. Zebrafish (*Danio rerio*) have been widely used

104 in Fish Embryo Toxicity (FET) Tests to assess the toxicity of several priority pollutants.

105 This embryonic bioassay has high sensitivity and low cost. Furthermore, zebrafish

106 embryos are translucent which allows for the monitoring of embryo development under

107 a stereomicroscope (Macedo et al., 2017; Zhang et al., 2015). This bioassay has recently

108 been proposed by the OECD as an alternative to classical acute fish toxicity tests

109 (Lammer et al., 2009), and is an appropriate tool to assess the decrease in toxicity after

110 treatment of wastewaters contaminated by emerging pollutants.

111 In this sense, embryo toxicity bioassays with zebrafish (*Danio rerio*) were used to

112 evaluate the initial effluent toxicity and possible attenuation of the toxic effect after the

113 UVC/H_2O_2 treatment by using the FluHelik reactor.

114 **2. Materials and methods**

115 *2.1 Chemicals*

116 Oxytetracycline hydrochloride (OTC, $C_{22}H_{24}N_2O_9$.HCl, 496.89 g/mol) was supplied by

117 Sigma-Aldrich and used as a model compound. Hydrogen peroxide (Fisher Chemical,

118 purity 49.5% (w/v)) was used as oxidant. Na_2SO_3 in a Na_2SO_3-to-H_2O_2 molar ratio of

119 1:1 was added to CECs and dissolved organic carbon (DOC) samples for H_2O_2

120 elimination (Jeong et al., 2010). Catalase (Sigma-Aldrich) was added to the samples to

121 eliminate residual H_2O_2 before performing ecotoxicological quality tests. Ammonium

122 monovanadate (Merck, p. a.) was used as colorimetric reagent to determine H_2O_2

123 concentration. Sulfuric acid (Pronalab, purity 96%, 1.84 g/cm^3) and sodium hydroxide

124   (Merck) were used for pH adjustment. Ultrapure water was obtained from a Millipore®

125   Direct-Q system (18.2 MΩ cm resistivity at 25 °C). Real wastewater sample was

126   collected downstream from the secondary treatment of an urban WWTP from Northern

127   Portugal in September 2017. Its physicochemical characteristics, including the CECs

128   residual concentrations detected in the raw effluent, are summarized in Table 1. The

129   ultrapure water and the secondary effluent both spiked with 20 mg OTC L^{-1} were used

130   as feed solutions. Table 2 shows the 11 pharmaceutical compounds added to the real

131   wastewater. Tricaine (1000 mg g^{-1}) used to anesthetize zebrafish larvae was purchased

132   from Pharmaq. Sodium hydrogen carbonate used as a buffer in the preparation of the

133   anesthetic was supplied by Merck KGaA. All the other chemicals supplied by VWR-

134   Prolabo, Sigma-Aldrich, Panreac, Merck, Fisher Scientific and Pronalab were either of

135   HPLC grade or analytical grade.

136   **Insert Table 1**

137   **Insert Table 2**

138   *2.2 Analytical determinations*

139   OTC concentration was followed by HPLC using a VWR Hitachi ELITE LaChrom LC

140   fitted with a Merck LiChrosorb® RP-18 (5 µm) LiChroCART® 125-4 column at 25 °C

141   and a diode array detector (DAD). Low-molecular-weight carboxylic acids (LMWCA)

142   concentrations were determined by ion-exclusion HPLC using the VWR Hitachi ELITE

143   LaChrom LC fitted with a Phenomenex RezexTM ROA-Organic Acid H+ (8%) 300

144   mm × 7.8 mm column at room temperature (25 ºC). A detailed description of OTC and

145   LMWCA analysis is given in Supplementary Material.

146   H_2O_2 concentration was determined by the colorimetric ($\lambda = 450$ nm) metavanadate

147   method (Nogueira et al., 2005). Dissolved organic carbon (DOC), chemical oxygen

148   demand (COD), total dissolved nitrogen, total dissolved iron, total suspended solids

149 (TSS), volatile suspended solids (VSS), total phosphorous, pH, temperature and

150 turbidity, as well as inorganic anions and cations concentrations were assessed

151 according to the procedures already described by Moreira et al. (2016)). Conductivity,

152 dissolved oxygen and redox potential were determined by a HANNA Instruments HI

153 9828 Multiparameter meter.

154 CECs determination in water samples, at residual concentrations, was performed in an

155 Acquity UPLC® liquid chromatograph system from Waters (Milford, MA, USA). A

156 sample volume of 45 μL was directly injected into a Luna C18 100A column (50 mm ×

157 2 mm, 3μm particle size) supplied by Phenomenex (Torrance, CA, USA) maintained at

158 a constant temperature of 30 °C. The target compounds were separated at a flow rate of

159 0.2 mL min^{-1} using 0.1% of formic acid in both, Milli-Q water (A) and MeOH (B) as

160 eluents. The applied gradient was as follows: 0–1 min, 0% B; 1–8 min, linear gradient

161 to 100% B; 7–13 min, 100% B and finally 13–20 min, 0% B. The system was interfaced

162 to a XEVO TQD® triple quadrupole mass spectrometer equipped with an electrospray

163 interface (ESI). Nitrogen was used as a nebulizing and drying gas and Argon was used

164 as collision gas. The analytes were determined in the electrospray (positive and negative

165 polarities) and multiple-reaction monitoring (MRM) mode of acquisition. Two MRM

166 transitions were used as quantifier and qualifier for each compound (see Table S1 for

167 detailed information). The method assured limits of quantification (LOQ) between 10

168 and 100 ng L^{-1} for all the compounds except for azytromicyn (LOQ 1.8 μg L^{-1}), see

169 supplementary material Table S1. Quantification was performed by the matrix matched

170 calibration method using standards prepared in treated wastewater in the 1-100 μg L^{-1}

171 (2-100 μg L^{-1} in the case of azytromicyn) range (which was checked to be linear,

172 R^2>0.99 for all the studied analytes). Repeatability of the determination was checked in

173 terms of relative standard deviation (RSD) at 10 μg L^{-1} level and the values were lower

174 than 10 % for all compounds.

175 *2.3 Experimental apparatus*

176 *2.3.1 Lab-scale*

177 The lab-scale system consists of: (i) a FluHelik stainless steel reactor or a Jets glass

178 reactor; (ii) a 1.5 or 5.5 L recirculation cylindrical glass vessel coupled to a thermostatic

179 bath (Julabo, model F12-EH) under magnetic stirring at 400 rpm (Velp Scientifica,

180 model T.ARE); (iii) a gear pump (Ismatec, model BVP-Z) to promote the fluid

181 recirculation. The system units were connected by polytetrafluoroethylene (PTFE)

182 tubing. Three low pressure mercury UVC lamps were used: (i) a 4 W power Philips

183 TUV G4T5, (ii) a 6 W power Philips TUV G6T5, and (iii) a 11 W power Philips TUV

184 G11T5. The photon flow for each photoreactor and respective UVC lamp power was

185 determined by H_2O_2 (73.5 mM) actinometry (Kuhn et al., 2004).

186 *2.3.1.1 Jets photoreactor*

187 The Jets reactor ($V_{illuminated}$ = 553 mL; light path-length = 40 mm) comprises (i) a

188 borosilicate glass cylindrical tube (d_{int} = 66 mm; length = 184 mm; thickness = 1.8 mm)

189 with four inlets and four outlets placed in parallel with the fluid flow at the ends of the

190 tube, and (ii) a concentric inner quartz tube (d_{ext} = 23 mm; length = 184 mm; thickness =

191 1 mm) filled with an UVC lamp. A scheme of the Jets photoreactor can be seen

192 elsewhere (Soares et al., 2016). Photonic fluxes of 0.8, 2.0 and 2.4 J_{UV} s^{-1} were

193 determined for 4, 6 and 11 W UVC lamps, respectively.

194 *2.3.1.2 FluHelik photoreactor*

195 The FluHelik reactor is an annular channel reactor consisting of (i) a cylindrical shell of

196 stainless steel (d_{int} = 72 mm; length = 186 mm; thickness = 2 mm), internally polished,

197 with inlet and outlet pipes located perpendicularly to the fluid flow and tangentially to

198   the shell in horizontal plane and at the top in opposite sides, and (ii) a concentric inner

199   quartz tube (d_{ext} = 23 mm; length = 186 mm; thickness = 1 mm) housing an UVC lamp

200   ($V_{illuminated}$ = 680 mL; light path-length = 46.0 mm). Fig. 1 displays the structure of this

201   reactor. The entire experimental unit was already fully described by Moreira et al.

202   (2019)). Photonic flow of 2.0 J_{UV} s^{-1} was determined for the 6 W UVC lamp.

<div align="center">**Insert Figure 1**</div>

204   *2.3.2 Pre-pilot scale - FluHelik*

205   The pre-pilot scale system consists of: (i) a FluHelik photoreactor made of a stainless

206   steel cylindrical shell (d_{int} = 154 mm; length = 480 mm; thickness = 7 mm), internally

207   polished, with tangential inlet and outlet; (ii) a concentric quartz tube (d_{out} = 49 mm;

208   length = 480 mm; thickness = 2 mm) to house a 95 W power Strahler UL C 2G11 UVC

209   lamp (19.3±0.3 J_{UV} s^{-1}; light path-length = 101.1 mm; $V_{illuminated}$ = 8.0 L); and (iii) a

210   cylindrical recirculation tank with 120 L capacity. The various components of the

211   system were connected by polypropylene (PP) tubing. The solution circulates

212   continuously by means of a centrifugal pump (GemmeCotti, model HTM15PP) at a

213   flow rate of 7500 L h^{-1} (Re = 15000) regulated by a rotameter.

214   *2.4 Experimental procedure*

215   *2.4.1 Assessment of OTC degradation*

216   A solution consisting of 5 or 20 mg L^{-1} of OTC in ultrapure water or urban wastewater

217   was added to a cylindrical glass vessel and homogenized by recirculation through all the

218   system during 10 min in the darkness. The temperature controller was switched on at a

219   temperature set-point that allowed preserving the inner solution at 25 ºC. A first control

220   sample was taken and then, the hydrogen peroxide was added and the UVC lamp was

221   switched on, stating the reaction beginning. Samples were taken at different time

222   intervals to evaluate the oxidation process. The OTC oxidation was evaluated using

223 different reaction conditions: i) direct photolysis (absence of oxidant), ii) only with

224 H_2O_2 (absence of radiation), iii) UVC/H_2O_2. The efficiency of the process was analyzed

225 by changing the H_2O_2 initial dosage (20-700 mg L^{-1}), the flow rate (50-100 L h^{-1}) and

226 the UVC lamp intensity (4, 6 or 11 W) at lab-scale and the H_2O_2 dosage (100-700 mg L^{-}

227 ^{1}) at pre-pilot scale. Both reactors (FluHelik and Jets) were operated in single pass and

228 in multiple pass flow mode. In single pass flow mode, the solution to be treated was

229 added to the glass vessel, followed by the hydrogen peroxide addition and homogenized

230 during 2 hours in the dark. A first control sample was taken and then the radiation

231 source was switched on, starting the reaction. Samples were collected at different time

232 periods until reaching the stationary phase. Immediately after samples collection,

233 Na_2SO_3 in a Na_2SO_3:H_2O_2 molar ratio of 1:1 was added to quench H_2O_2.

234 The photochemical space time yield (PSTY, m^3$_{water}$ m^{-3}$_{reactor}$ day^{-1} kW^{-1}) was calculated

235 via Eq. (1) (Leblebici et al., 2015).

236 $$PSTY = \frac{STY}{LP} \tag{1}$$

237 Where the space-time yield (STY, m^3$_{water}$ m^{-3}$_{reactor}$ day^{-1}) is standardized to the volume

238 (m^3) of the wastewater processed from 20 mg L^{-1} to 0.02 mg L^{-1} of OTC (three orders of

239 magnitude) in a 1 day by the reactor when it is scaled up to 1 m^3 (V_R). STY can be

240 calculated from the apparent reaction rate k (day^{-1}), considering the FluHelik reactor

241 operated in a loop as a continuous stirred tank reactor (Eq. 3).

242 $$C_A = \frac{C_{A_0}}{1 + k\tau} \tag{2}$$

243 where C_A is the outlet concentration in mg L^{-1}, C_{A_0} is the inlet concentration in mg L^{-1}

244 and τ is the passage time in days. From Eq. 3, τ can be calculated and used to determine

245 the STY, according to Eq. 4.

246 $$STY = \frac{V_R}{\tau} = \frac{1m^3}{\tau} = \frac{k}{999} \tag{3}$$

247   In its turn, *LP* (kW) is the standardized lamp power, which would illuminate 1 m^3 of the

248   reactor, where the lamp power (*P*) in kW is normalized to the volume (*V*, m^3) of the

249   reaction medium in the experimental setup (Eq. 4).

250    $$LP = P\frac{1m^3}{V} \hspace{8cm} (4)$$

251   *2.4.2 Assessment of CECs degradation*

252   An urban wastewater fortified with 60 μg L^{-1} of OTC and 10 additional CECs (present

253   in Table 2) from the 12 established by the Swiss legislation (Hochstrat et al., 2015) was

254   added to a cylindrical glass vessel and homogenized by recirculation through all the

255   system during 10 min in the darkness. The temperature controller was switched on at a

256   temperature set-point that allowed preserving the inner solution at 25 ºC. A first control

257   sample was taken and then, the hydrogen peroxide was added and the 6 W UVC lamp

258   was switched on, stating the reaction beginning. Samples were taken after 30 min of

259   reaction to evaluate the oxidation process. The efficiency of the process was analyzed

260   by changing the H$_2$O$_2$ initial dosage (10-500 mg L^{-1}) using the lab-scale FluHelik

261   photoreactor at a flow rate of 100 L h^{-1} and pH 7.5. The system was operated in single

262   pass and in multiple pass flow mode. Immediately after samples collection, catalase

263   solution was added to quench H$_2$O$_2$.

264   *2.5 Toxicity screening with zebrafish embryo bioassays*

265   Zebrafish embryo bioassays were used to evaluate the efficiency of the UVC/H$_2$O$_2$

266   photochemical system with the FluHelik photoreactor in reducing the toxicity of the

267   UWW spiked with 11 CECs (Table 1 and 2). The bioassays included the exposition of

268   zebrafish embryos to the UWW spiked with trace level of 11 CECs before (UWW + 11

269   CECs) and after treatment (UWW + 11 CECs + Treatment). The toxicity of the UWW

270   without the CECs addition (UWW) was also assessed.

271   *2.5.1 Fertilization and embryos collection*

272   A stock of adults zebrafish were maintained in 150 L aquarium with dechlorinated

273   filtered and aerated water at 28 ± 1 °C, under a photoperiod of 14:10 h (light:dark). The

274   animals were fed two times per day with commercial fish diet Tetramin (Tetra, Melle,

275   Germany) supplemented with *Artemia spp* (Barros et al., 2018). For the zebrafish

276   reproduction, in the afternoon before breeding, a group of males and females (2:1) was

277   isolated in a breeding box under the same water and photoperiod conditions as the

278   stock. At the following day, 1.5 h after the beginning of the light period the eggs were

279   collected and cleaned to be used in the zebrafish embryo bioassays (Barros et al., 2018;

280   Ribeiro et al., 2015; Torres et al., 2016).

281   *2.5.2 Zebrafish embryo bioassays*

282   The bioassays were carried out with slight modification of OECD Fish Embryo Acute

283   Toxicity (FET) Test 236 (Barros et al., 2018; OECD, 2013). After observation in a

284   magnifying glass, cleaned fertilized embryos were randomly allocated into 24-wells

285   plates (one embryo per well) filled with 2 mL of freshly solutions and control. The

286   experiments consisted of 5 treatments of 20 embryos each divided in six replicates:

287   UWW, UWW + 11 CECs, UWW + 11 CECs + Treatment and Control (dechlorinated

288   water). In each 24-well plate was allocated one treatment (20 embryos) plus an internal

289   plate control (4 embryos) (Fig. S1).

290   The 24-well plates were randomly maintained on a water bath at 26.5 ± 0.5 °C for 80 h.

291   Embryos were checked, every day, for mortality and dead embryos were removed. The

292   medium was renewed daily in order to maintain oxygen and the integrity of the

293   solutions. At the end of the bioassay (80 hpf), under an inverted microscope (Nikon

294   Eclipse 5100T) equipped with a digital camera (Nikon D5-Fi2), morphological

295   abnormalities on tail or yolk-sac; pericardial oedema and lordosis were recorded as

296   present or absent (Fig. S2) (Barros et al., 2018). The different abnormalities' were

297   grouped and presented as total abnormalities. At the same time the length and the yolk

298   sac perimeter of 10 larvae per treatment were recorded.

299   *2.5.3 Statistical analysis*

300   Data were first checked for homogeneity of variances (Levene's test) and subsequently

301   analyzed by one-way ANOVA followed by Fisher's least significant difference test

302   (LSD) or nonparametric analysis (Kruskall-Wallis ANOVA by ranks followed by

303   multiple comparisons of mean ranks). The significance threshold was set at $p < 0.05$.

304   All statistics were computed with Statistica (Stat-soft, USA).

305   **3. Results and discussion**

306   *3.1 OTC degradation by an UVC/H_2O_2 photochemical system using a conventional Jets*

307   *photoreactor in multiple pass flow mode*

308   Initially it was assessed the effect of pH on the direct photolysis of 5 mg L^{-1} of OTC

309   with an UVC lamp of 6 W. OTC removals of 82 and 88% after 120 min were achieved

310   at pH 4.5 and 7.5, respectively, without pH control during the experiments. No

311   significant pH variations were observed for the experiments performed at OTC solution

312   pH (4.5). However, the solution pH decreased to values below 6.5 during the

313   experiments performed at an initial pH of 7.5. On the other hand, the OTC removal

314   increased to 98% only after 60 min when the solution pH was controlled at 7.5 through

315   the addition of NaOH solution. For pH values higher than 6.5, the predominant OTC

316   species are negative, which are more susceptible to photochemical degradation (Liu et

317   al., 2015).

318   In order to follow the reaction kinetics in a more rigorously way, a synthetic solution

319   with 20 mg OTC L^{-1} was used in the next experiments. OTC removals above 90% were

320   achieved after 120 and 90 min of reaction under direct photolysis using a 4 and 6 or 11

321   W UVC lamp, respectively. On the other hand, the OTC removal proved also to be

322 possible by H_2O_2 in the absence of radiation, attaining degradations of 20, 30 and 50%

323 after 180 min of reaction using 100, 300 and 500 mg L^{-1} of oxidant, respectively. As

324 expected, the combination of UVC light with H_2O_2 improved the OTC degradation

325 under all the studied irradiation intensities (Fig. 2). It is noteworthy that the

326 photochemical oxidation of OTC showed to follow a pseudo-first order kinetic model.

327 For all the UVC lamp intensities evaluated, the OTC removal rates increased with the

328 initial oxidant dose, attaining the highest removal rates (see pseudo-first order kinetic

329 constants, k, in Table 3) with 100 mg L^{-1} when using the 4 or the 6 W lamps (Fig. 2a

330 and 2b, respectively) and with 500 mg L^{-1} of H_2O_2 when the 11 W UVC lamp (Fig. 2c)

331 was employed (within the tested concentrations range). These results suggest an

332 increasing production of hydroxyl radicals ($^\bullet$OH) for growing H_2O_2 initial contents (H.

333 Baxendale and A. Wilson, 1957). For higher oxidant dosages, the reaction rates

334 remained constant and, for the 11 W lamp there was even a decrease of 1.3 times in the

335 kinetic constant when using 700 mg L^{-1} of H_2O_2 (Table 3). In fact, the H_2O_2 in excess

336 can act as an hydroxyl radicals scavenger (Muruganandham and Swaminathan, 2004).

337 This is supported by the growing H_2O_2 consumption for rising initial H_2O_2 doses (Fig.

338 2).

339 **Insert Figure 2**

340 **Insert Table 3**

341 Comparing the OTC removals by the UVC/H_2O_2 system under the best conditions for

342 each of the lamp powers studied (Fig. 2d), no significant differences between the

343 reaction rates (in terms of energy) were observed. For all the systems, an OTC removal

344 above 90% is already achieved with 0.4 kJ L^{-1}. On the other hand, a different behaviour

345 was observed in relation to the OTC mineralization: DOC decays of 13, 50 and 45%

346 after 60 min of reaction were observed at the best conditions when using the 4, 6 and 11

347 W lamps, respectively. It is worth mentioning that, during this reaction period, similar

348 oxidant consumptions were noticed for the 4 and 6 W lamps (c.a. 35 mg H_2O_2 L^{-1});

349 however, when using the 11 W lamp a 5-fold increase in hydrogen peroxide

350 consumption (higher initial H_2O_2 dose) was observed. These results prove that the

351 higher H_2O_2 consumption associated to the 11 W lamp is not related with a higher

352 mineralization, but probably to parasite reactions. Therefore, the 6 W lamp provided the

353 most suitable photon flow for the experimental set-up used: the 4 W lamp showed to not

354 supply the necessary UV dosage and, in turn, using the 11 W UVC lamp a possible loss

355 of the emitted photons is occurring, probably due to the low molar absorption

356 coefficient of H_2O_2 at 254 nm, requiring higher amounts of H_2O_2 to absorb all those

357 photons.

358 As above-mentioned, although the total degradation of the parent compound (OTC) is

359 achieved in short reaction times, relatively low mineralization is observed. Actually, for

360 longer reaction times (360 min), a mineralization of 62% was reached (6 W UVC lamp;

361 100 mg H_2O_2 L^{-1}), consuming 87 mg L^{-1} hydrogen peroxide, a higher value than the one

362 predicted by the reaction stoichiometry to completely mineralize 20 mg L^{-1} of OTC (77

363 mg H_2O_2 L^{-1}). In fact, 38% of the residual DOC corresponds to low-molecular-weight

364 carboxylic acids (LMWCA) in solution, namely oxalic and oxamic acids.

365 The H_2O_2/UVC process led to higher OTC degradation rates with the increment of Q

366 from 50 to 100 L h^{-1} (Table 3), indicating a change in the hydrodynamic conditions

367 inside the photoreactor. A Re number of 446 ($Q = 100$ L h^{-1}) allowed to a 2.3-fold

368 increase on OTC oxidation rate comparing with a Re of 223 ($Q = 50$ L h^{-1}). At those

369 conditions, an OTC removal above 90% is achieved after 5 min of reaction with 0.4 kJ

370 L^{-1}.

3.2 OTC degradation by an UVC/H$_2$O$_2$ photochemical system using an innovative FluHelik photoreactor in multiple pass flow mode

An initial H$_2$O$_2$ dose of 300 mg L^{-1} led to a maximum OTC oxidation rate and mineralization, corresponding to a 9-fold increment on reaction rate when compared to direct photolysis (Table 3). A higher oxidant dose (400 mg L^{-1}) led to a slightly decrease in the OTC oxidation rate, due to hydroxyl radicals quenching by the hydrogen peroxide molecule itself. This is also supported by the growing H$_2$O$_2$ consumption for rising initial H$_2$O$_2$ doses (Fig. 3). Using 300 mg L^{-1} of oxidant, a 77% mineralization was attained after 360 min with a final residual H$_2$O$_2$ concentration of 17 mg L^{-1}. 50% of the remaining DOC was from oxalic and oxamic acids. In turn, the nitrogen content of the OTC compound was converted to nitrites, nitrates and ammonium, with ammonia representing the largest fraction. The un-mineralized fraction of nitrogen proved to be present as oxamic acid, as also observed by Pereira et al. (2013)).

Insert Figure 3

The OTC removal rate showed a 1.6-fold increase when the flow rate increased from 50 to 75 L h^{-1}. A further increase on flow rate from 75 to 100 L h^{-1} resulted in an increment on the reaction rate of only 1.2 times (see Table 3). This indicates that the hydrodynamic conditions do not considerably change between 75 to 100 L h^{-1}. Under this condition (100 L h^{-1}), an OTC removal >90% is reached after 5 min of reaction (0.4 kJ L^{-1} of accumulated energy), with a photonic efficiency (ξ) (number of OTC transformed molecules divided by the number of incident photons) of 13.7%.

Comparing the degradation of the OTC molecule in UPW matrix by the two reactors under study in the best conditions found for each one (Fig. 4), it was practically similar in both reactors. On the other hand, FluHelik reactor showed to be more efficient (1.3 times) in terms of mineralization (77%) when compared with the Jets reactor (61%), for

16

396   the same accumulated UVC energy (14.4 kJ_{UV} L^{-1}). This indicates that the limiting step

397   of the reaction is the by-products removal, which is improved by the unique fluid

398   dynamics and irradiation properties of FluHelik reactor.

399   **Insert Figure 4**

400   *3.3 Effect of urban wastewater (UWW) matrix*

401   OTC removal by the UVC/H_2O_2 photochemical system was also evaluated for an UWW

402   fortified with 20 mg OTC L^{-1}. Fig. 5a shows an increment on OTC removal rate for

403   higher H_2O_2 doses using the Jets photoreactor. In fact, a 29-fold increase on OTC

404   oxidation rate is observed for the UVC/H_2O_2 system ($[H_2O_2]_0$ = 500 mg L^{-1}) when

405   compared to direct photolysis (Table 3). Likewise, it was found that the highest OTC

406   oxidation rate using the UWW and the FluHelik photoreactor was reached with the

407   highest oxidant concentration applied ($[H_2O_2]_0$ = 500 mg L^{-1}) (Fig 5b, Table 3). An

408   increase in the flow rate value from 50 to 100 L h^{-1}, achieved a 1.2-fold improvement in

409   the OTC reaction rate (Table 3), associated with an higher degree of mixing inside the

410   system. Under those conditions (500 mg H_2O_2 L^{-1}; 100 L h^{-1}), 90% of OTC removal

411   was achieved after 7.5 min of reaction and using 0.6 kJ_{UV} L^{-1} and a final mineralization

412   of 71% was attained after 180 min of reaction and 14.4 kJ_{UV} L^{-1}. Paralleling the reaction

413   rates in both matrices, a decrease of about 1.7 times was perceived when in the presence

414   of the UWW, using the same initial H_2O_2 dosage, mainly due to inner filter and

415   hydroxyl radicals scavenging effects (Wols and Hofman-Caris, 2012). Therefore, a

416   higher amount of oxidant is required to overcome those effects to obtain similar OTC

417   removals. In fact, when using the FluHelik photoreactor for both matrices, at the best

418   conditions, similar photochemical space time yield (PSTY) were observed (0.50 and

419   0.53 m^3_{water} $m^{-3}_{reactor}$ day^{-1} kW^{-1} using the UPW and UWW, respectively). This shows

420   the ability of the FluHelik reactor design to overcome matrix effects due to its unique

                                                                                                    17

421   characteristics. It should be noted that the high H_2O_2 concentrations used in these

422   experiments were due to the low photon flows provided by the available UVC lamps. If

423   higher photon flows are provided (able of overcoming the wastewater inner filter

424   effects), lower initial doses of oxidant would be required to achieve the same OTC

425   oxidation rates.

426   **Insert Figure 5**

427   The FluHelik photoreactor showed a better performance than the conventional Jets

428   reactor during the OTC oxidation when in the presence of the UWW matrix at the same

429   operating conditions (500 mg L^{-1} of H_2O_2 and 100 L h^{-1}) (Fig. 6, Table 3). In this case,

430   the helical movement of the fluid around the radiation source allows a more

431   homogeneous UV radiation distribution, enhancing the reaction rate. In fact, the Jets

432   reactor presents a solution flow pattern parallel to the radiation source, and

433   consequently, the liquid streams at higher distance from the light source receive a less

434   UV dose. FluHelik's unique fluid hydrodynamics also provided a more efficient oxidant

435   homolytic cleavage, allowing further removal of the remaining by-products. In fact, a

436   1.4 times higher hydrogen peroxide consumption was observed when using the

437   FluHelik reactor (Fig. 6), reaching a mineralization of 71% instead of 56% for the Jets

438   reactor, using the same accumulated UVC energy (14.4 kJ_{UV} L^{-1}).

439   **Insert Figure 6**

440   The FluHelik photoreactor was also evaluated for the treatment of an UWW matrix

441   spiked with OTC and 10 additional CECs (described in Table 2) from the 12 established

442   by Swiss legislation (Hochstrat et al., 2015) at residual concentrations (60 µg L^{-1}) using

443   the UVC/H_2O_2 photochemical process. The Swiss legislation establishes 80% removal

444   for 5 out of 12 indicator compounds (11 pharmaceuticals and 1 biocide) (Hochstrat et

445   al., 2015). An OTC removal of more than 80% can be achieved using only 10 mg L^{-1} of

446 H_2O_2 (Table 2) after 30 min. In order to comply with the Swiss legislation, an oxidant

447 amount of 250 mg L^{-1} is required to achieve 80% removal of 5 compounds after 30 min.

448 However, using a H_2O_2 dose of 500 mg L^{-1}, after 30 min of reaction, a removal

449 efficiency of 80% is obtained for all the 11 CECs.

450 *3.4 CECs removal by an UVC/H_2O_2 photochemical system using FluHelik/Jets*

451 *photoreactors in single pass flow mode*

452 In order to estimate the efficiency in a real scale implementation, tests were performed

453 in single pass flow mode (one passage through the reactor) instead of recirculating the

454 solution between the reactor and the feed tank (multiple passage). In this way it is also

455 ensured that only the hydrodynamic effect of the reactors is evaluated, excluding the

456 additional mixture promoted by the recirculation. Fig 7a shows an improvement on the

457 OTC removal from an UWW matrix, at the steady state conditions (5 times the

458 residence time), by the UVC/H_2O_2 process (500 mg H_2O_2 L^{-1}; 6 W; 100 L h^{-1}), using the

459 FluHelik photoreactor (18% OTC removal) instead of the Jets reactor (15% OTC

460 removal). In fact, the longer residence time of FluHelik reactor (0.4 min) when

461 compared to that of the Jets reactor (0.3 min), along with the higher accumulated energy

462 (in a single passage) and with the lower dead volume zones due to the FluHelik helical

463 movement of the fluid contributed to the higher OTC removal.

464 Table 2 shows that much smaller removals of all the 11 CECs spiked in the UWW were

465 achieved by operating the FluHelik reator in single passage mode (low residence time):

466 none of the compounds reach the removal imposed by Swiss legislation. The design of

467 the FluHelik photoreactor strongly favors the implementation of various reactors in

468 series, promoting its application in industry. Therefore, two FluHelik photoreactors

469 associated in series were tested for the removal of 20 mg L^{-1} of OTC under the same

470 conditions previously tested with only one reactor. However, it was noticed that when

471 using the two reactors in series an OTC removal of only 31% was obtained after

472 reaching the steady state (Fig. 7b), a lower value than the one expected (36% - twice the

473 one achieved with only one reactor). In fact, when using 2 FluHelik reactors in series,

474 different velocity profiles can be found in the each reactor due to an increase in fluid

475 energy dissipation (pressure drop). Therefore, a new test was carried out doubling the

476 flow rate (200 L h^{-1}), corresponding to a residence time of 0.4 min. At these conditions,

477 an OTC removal of 36% was attained at steady state conditions. Therefore, when using

478 2 FluHelik reactors in series there is a minimum flow rate value to be used to achieve

479 fluid velocities profiles inside both photoreactors similar to when using only one

480 FluHelik reactor.

481 **Insert Figure 7**

482 Finally, a pilot-scale FluHelik reactor (95 W UVC lamp) under multiple pass flow mode

483 was also evaluated for the OTC removal using either UPW and UWW as solution

484 matrices. This system was operated at a flow rate of 7500 L h^{-1}, attaining a turbulent

485 regime inside the photoreactor (Re = 15000). Fig. 8a and 8b show that the highest OTC

486 oxidation rate was reached when using 500 mg L^{-1} of H_2O_2 for both reaction matrices.

487 However, a 1.5-fold decrease in the OTC kinetic rate (Table 3) was obtained for the

488 UWW when compared with UPW, as well as a slightly lower mineralization (52%

489 instead of 58%) using 4.6 kJ$_{UV}$ L^{-1}. It should be noted that, at the best conditions, when

490 using UPW, a higher photochemical space time yield (PSTY) at pre-pilot scale (0.85

491 m$^3_{water}$ m$^{-3}_{reactor}$ day^{-1} kW^{-1}) when compared with the one at lab scale (0.50 m$^3_{water}$

492 m$^{-3}_{reactor}$ day^{-1} kW^{-1}) was noticed. This dissimilarity is mainly associated to the different

493 flow rates and UV fluence inside the reactors (distinct path length and UVC lamp

494 power). In addition, when using UWW, similar PSTY were observed at both scales

495 (0.57 and 0.53 m$^3_{water}$ m$^{-3}_{reactor}$ day^{-1} kW^{-1} at the pre-pilot scale and lab scale,

496   respectively). These data are in agreement with the results obtained by Moreira et al.

497   (2019)) when comparing the degradation of a model compound, 3-amino-5-

498   methylisoxazole, using the FluHelik at the lab and pre-pilot scale; and indicate the

499   feasibility of scaling-up the FluHelik reactor.

500   **Insert Figure 8**

501   *3.5 Toxicity*

502   The percentage of embryo mortality at the end of the bioassays was similar among

503   treatments and remained at low levels, below 3% (data not shown). The total

504   abnormalities, the length and the yolk sac perimeter observed on zebrafish embryos

505   exposed to the initial and treated effluents are presented in Fig. 9. A significant increase

506   of total abnormalities (sum of tail abnormalities, lordosis anomalies and pericardial

507   oedema) was observed in embryos exposed to the UWW + 11 CECs, with 12.5% of

508   abnormal embryos in comparison with 1.4% of the control ($p < 0.05$). These

509   abnormalities were significantly reduced after the FluHelik photochemical treatment

510   (UWW + 11 CECs + Treatment), with values similar to the control (4.7% - $p > 0.05$).

511   The exposure to the UWW without the 11 CECs addition did not cause significant

512   abnormalities in the embryos ($p > 0.05$).

513   **Insert Figure 9**

514   It was also verified that the exposure to the UWW + 11 CECs significantly decreased

515   the length of the larvae and increase the yolk sac perimeter when compared with control

516   ($p < 0.05$). These endpoints return to control levels after the FluHelik photochemical

517   treatment (UWW + 11 CECs + Treatment). The yolk sac perimeter was also

518   significantly increased by the UWW without the 11 CECs.

519   When comparing the toxicity effects of the UWW + 11 CECs with those of the UWW +

520   11 CECs + Treatment (Fig. 9), it is evident that the UVC/H_2O_2 photochemical system

521 using the FluHelik photoreactor led to a significant decrease of the toxicity on zebrafish

522 embryos. In this sense, the treated wastewater had no significant effects on the total

523 abnormalities incidence, in the length of the larva and in the yolk sac perimeter. Thus, it

524 may be assumed that the degradation of pollutants present in the UWW fortified with 11

525 CECs by the UVC/H_2O_2 photochemical system with the FluHelik photoreactor did not

526 result in toxic transformation products to zebrafish embryos.

527 **4. Conclusions**

528 The FluHelik photoreator showed to be an interesting system for UVC/H_2O_2

529 photochemical process applied to the removal of CECs from urban wastewaters, as a

530 polishing step, being able to to comply with the Switzerland legislation and to

531 effectively reduce CECs toxicity to zebrafish embryos. Due to its unique configuration,

532 the FluHelik promotes an helical movement of the fluid around the irradiation source,

533 providing a more homogeneous UV radiation distribution (each fluid particle receives a

534 similar UVC radiation dosage), being able to overcome matrix effects in wastewaters

535 with low to moderate transmissibility (inner filter effects). Another advantage of this

536 reactor technology is its easy scalability, through its very simple and compact

537 arrangement in series, strongly promoting its use in industrial applications.

546 **References**

547 Barros S, Montes R, Quintana JB, Rodil R, André A, Capitão A, et al. Chronic
548　　environmentally relevant levels of simvastatin disrupt embryonic development,
549　　biochemical and molecular responses in zebrafish (Danio rerio). Aquatic
550　　Toxicology 2018; 201: 47-57.
551 Boyjoo Y, Ang M, Pareek V. CFD simulation of a pilot scale slurry photocatalytic
552　　reactor and design of multiple-lamp reactors. Chemical Engineering Science
553　　2014; 111: 266-277.
554 Cambié D, Bottecchia C, Straathof NJW, Hessel V, Noël T. Applications of
555　　Continuous-Flow Photochemistry in Organic Synthesis, Material Science, and
556　　Water Treatment. Chemical Reviews 2016; 116: 10276-10341.
557 Caris CHM. New concepts of UV/H_2O_2 oxidation: KWR, 2011.
558 Diya'uddeen BH, Daud WMAW, Abdul Aziz AR. Treatment technologies for
559　　petroleum refinery effluents: A review. Process Safety and Environmental
560　　Protection 2011; 89: 95-105.
561 H. Baxendale J, A. Wilson J. The Photolysis of Hydrogen Peroxide at High Light
562　　Intensities. Vol 53, 1957.
563 Hochstrat R, Scharer M, Bleny H. Elimination of micropollutants – the Swiss approach.
564　　TAPES Final Conference, Brussels, 2015.
565 Jeong J, Song W, Cooper WJ, Jung J, Greaves J. Degradation of tetracycline antibiotics:
566　　Mechanisms and kinetic studies for advanced oxidation/reduction processes.
567　　Chemosphere 2010; 78: 533-540.
568 Karpel VelLeitner N, Le Bras E, Foucault E, Bousgarbies JL. A new photochemical
569　　reactor design for the treatment of absorbing solutions. Water Science and
570　　Technology 1997; 35: 215-222.
571 Krishnan S, Rawindran H, Sinnathambi CM, Lim JW. Comparison of various advanced
572　　oxidation processes used in remediation of industrial wastewater laden with
573　　recalcitrant pollutants. IOP Conference Series: Materials Science and
574　　Engineering 2017; 206: 012089.
575 Kuhn HJ, Braslavsky SE, Schmidt R. Chemical actinometry (IUPAC Technical Report).
576　　Pure and Applied Chemistry. 76, 2004, pp. 2105.
577 Lammer E, Carr GJ, Wendler K, Rawlings JM, Belanger SE, Braunbeck T. Is the fish
578　　embryo toxicity test (FET) with the zebrafish (Danio rerio) a potential
579　　alternative for the fish acute toxicity test? Comparative Biochemistry and
580　　Physiology Part C: Toxicology & Pharmacology 2009; 149: 196-209.
581 Leblebici ME, Stefanidis GD, Van Gerven T. Comparison of photocatalytic space-time
582　　yields of 12 reactor designs for wastewater treatment. Chemical Engineering and
583　　Processing: Process Intensification 2015; 97: 106-111.
584 Liu Y, He X, Duan X, Fu Y, Dionysiou DD. Photochemical degradation of
585　　oxytetracycline: Influence of pH and role of carbonate radical. Chemical
586　　Engineering Journal 2015; 276: 113-121.
587 Macedo S, Torres T, Santos MM. Methyl-triclosan and triclosan impact embryonic
588　　development of Danio rerio and Paracentrotus lividus. Ecotoxicology 2017; 26:
589　　482-489.
590 Masschelein WJ. Ultraviolet disinfection of water. In : Unit Processes in Drinking
591　　Water Treatment. Vol Chap. 4, 1992.

592 Moreira FC, Bocos E, Faria AGF, Pereira JBL, Fonte CP, Santos RJ, et al. Selecting the
593　　best piping arrangement for scaling-up an annular channel reactor: An

594   experimental and computational fluid dynamics study. Science of the Total
595   Environment 2019; (Accepted).
596 Moreira FC, Soler J, Alpendurada MF, Boaventura RAR, Brillas E, Vilar VJP. Tertiary
597   treatment of a municipal wastewater toward pharmaceuticals removal by
598   chemical and electrochemical advanced oxidation processes. Water Research
599   2016; 105: 251-263.
600 Muruganandham M, Swaminathan M. Photochemical oxidation of reactive azo dye with
601   UV–H_2O_2 process. Dyes and Pigments 2004; 62: 269-275.
602 Noël T. Photochemical Processes in Continuous-Flow Reactors. New Jersey: World
603   Scientific Publishing Europe Ltd., 2017.
604 Nogueira RFP, Oliveira MC, Paterlini WC. Simple and fast spectrophotometric
605   determination of H_2O_2 in photo-Fenton reactions using metavanadate. Talanta
606   2005; 66: 86-91.
607 OECD. Test No. 236: Fish Embryo Acute Toxicity (FET) Test, 2013.
608 Pereira JHOS, Reis AC, Queirós D, Nunes OC, Borges MT, Vilar VJP, et al. Insights
609   into solar TiO_2-assisted photocatalytic oxidation of two antibiotics employed in
610   aquatic animal production, oxolinic acid and oxytetracycline. Science of The
611   Total Environment 2013; 463-464: 274-283.
612 Ribeiro S, Torres T, Martins R, Santos MM. Toxicity screening of Diclofenac,
613   Propranolol, Sertraline and Simvastatin using Danio rerio and Paracentrotus
614   lividus embryo bioassays. Ecotoxicology and Environmental Safety 2015; 114:
615   67-74.
616 Soares PA, Silva TFCV, Ramos Arcy A, Souza SMAGU, Boaventura RAR, Vilar VJP.
617   Assessment of AOPs as a polishing step in the decolourisation of bio-treated
618   textile wastewater: Technical and economic considerations. Journal of
619   Photochemistry and Photobiology A: Chemistry 2016; 317: 26-38.
620 Su Y, Straathof NJW, Hessel V, Noël T. Photochemical Transformations Accelerated in
621   Continuous-Flow Reactors: Basic Concepts and Applications. Chemistry – A
622   European Journal 2014; 20: 10562-10589.
623 Subramanian M, Kannan A. Photocatalytic degradation of phenol in a rotating annular
624   reactor. Chemical Engineering Science 2010; 65: 2727-2740.
625 Torres T, Cunha I, Martins R, Santos M. Screening the Toxicity of Selected Personal
626   Care Products Using Embryo Bioassays: 4-MBC, Propylparaben and
627   Triclocarban. International Journal of Molecular Sciences 2016; 17: 1762.
628 Wols BA, Hofman-Caris CHM. Review of photochemical reaction constants of organic
629   micropollutants required for UV advanced oxidation processes in water. Water
630   Research 2012; 46: 2815-2827.
631 Yatmaz HC, Wallis C, Howarth CR. The spinning disc reactor – studies on a novel
632   TiO2 photocatalytic reactor. Chemosphere 2001; 42: 397-403.
633 Zhang Q, Cheng J, Xin Q. Effects of tetracycline on developmental toxicity and
634   molecular responses in zebrafish (Danio rerio) embryos. Ecotoxicology 2015;
635   24: 707-719.
636
637

Figure Captions

Fig. 1. FluHelik photoreactor scheme.

Fig. 2. Effect of H_2O_2 initial concentration and respective consumption ($\blacktriangledown$ - Direct photolysis; $\blacksquare$ - 20 mg H_2O_2 L^{-1}; $\bullet$ - 50 mg H_2O_2 L^{-1}; $\blacktriangle$ - 100 mg H_2O_2 L^{-1}; $\blacktriangleleft$ - 200 mg H_2O_2 L^{-1}; $\blacktriangleright$ - 500 mg H_2O_2 L^{-1}; $\blacklozenge$ - 700 mg H_2O_2 L^{-1}) on the degradation of OTC ($[OTC]_0$ = 20 mg L^{-1}) by a UVC/H_2O_2 process with (a) 4 W, (b) 6 W and (c) 11 W UVC lamp; (d) OTC removal profiles at the optimized H_2O_2 concentrations for each lamp ($\blacksquare$ - 4W lamp and 100 mg H_2O_2 L^{-1}; $\bullet$ - 6W lamp and 100 mg H_2O_2 L^{-1}; $\blacktriangle$ - 11W lamp and 500 mg H_2O_2 L^{-1}): Jets reactor; multiple pass flow mode; Q = 100 L h^{-1}, pH 7.5 and 25 ºC.

Fig. 3. Effect of H_2O_2 initial concentration and respective consumption ($\blacktriangledown$ - Direct photolysis; $\blacksquare$ - 100 mg H_2O_2 L^{-1}; $\bullet$ - 200 mg H_2O_2 L^{-1}; $\blacktriangle$ - 300 mg H_2O_2 L^{-1}; $\blacktriangleleft$ - 400 mg H_2O_2 L^{-1}) on the degradation of OTC by a UVC/H_2O_2 process using the FluHelik photoreactor: $[OTC]_0$ = 20 mg L^{-1}; Q = 100 L h^{-1}; multiple pass flow mode; 6 W UVC lamp, pH 7.5 and 25 ºC.

Fig. 4. OTC removal from a ultrapure water matrix by a UVC/H_2O_2 process, as well as H_2O_2 consumption and mineralization efficiencies (open symbols) achieved when using the ($\blacksquare$) Jets reactor with 100 mg L^{-1} of H_2O_2 and ($\bullet$) the FluHelik reactor with 300 mg L^{-1} of H_2O_2: $[OTC]_0$ = 20 mg L^{-1}, Q = 100 L h^{-1}; multiple pass flow mode; 6 W UVC lamp; pH 7.5 and 25 ºC.

Fig. 5. Effect of H_2O_2 initial concentration and respective consumption ($\blacktriangledown$ - Direct photolysis; $\blacksquare$ - 100 mg H_2O_2 L^{-1}; $\bullet$ - 300 mg H_2O_2 L^{-1}, $\blacktriangle$ - 500 mg H_2O_2 L^{-1}) on the degradation of OTC in a real urban wastewater matrix using a UVC/H_2O_2 process with (a) a Jets reactor and (b) a FluHelik reactor: $[OTC]_0$ = 20 mg L^{-1}; Q = 100 L h^{-1}; multiple pass flow mode; 6 W UVC lamp; pH 7.5 and 25 ºC.

Fig. 6. OTC removal from a real urban wastewater by a UVC/H_2O_2 process, as well as H_2O_2 consumption and mineralization efficiencies (open symbols) achieved when using ($\blacksquare$) the Jets reactor and ($\bullet$) the FluHelik reactor: $[OTC]_0$ = 20 mg L^{-1}; Q = 100 L h^{-1}; multiple pass flow mode; 6 W UVC lamp; $[H_2O_2]$ = 500 mg L^{-1}; pH 7.5 and 25 ºC.

672

Fig. 7. OTC removal from a real urban wastewater by a UVC/H_2O_2 process using (a) the Jets reactor (■) and the FluHelik reactor (●) at 100 L h^{-1} and (b) 1 FluHelik reactor at 100 L h^{-1} (■), 2 FluHelik reactors in series at 100 L h^{-1} (●), 2 FluHelik reactors in series at 200 L h^{-1} (▲): [OTC]$_0$ = 20 mg L^{-1}; single pass flow mode; 6 W UVC lamp; [H_2O_2] = 500 mg L^{-1}; pH = 7.5 and 25ºC.

678

Fig. 8. Effect of H_2O_2 initial concentration and respective consumption (■ - 100 mg H_2O_2 L^{-1}; ● - 300 mg H_2O_2 L^{-1}; ▲ - 500 mg H_2O_2 L^{-1}; ◄ - 700 mg H_2O_2 L^{-1}) on the degradation of OTC in (a) a ultrapure water matrix and (b) a real urban wastewater matrix by a UVC/H_2O_2 process using a FluHelik reactor at pilot-scale: [OTC]$_0$ = 20 mg L^{-1}; Q = 7500 L h^{-1}; multiple pass flow mode; 95 W UVC lamp; pH = 7.5 and 25ºC.

684

Fig. 9. (a) Total abnormalities (%) and (b) larval length (■) and yolk sac (▢) perimeter (%) of *Danio rerio* embryos exposed to a real urban wastewater containing 11 pharmaceuticals before (UWW + 11 CECs) and after (UWW + 11 CECs + Treatment) the UVC/H_2O_2 treatment in the FluHelik photoreactor plus the real urban wastewater (UWW) without the 11 pharmaceuticals. Results are normalized to the respective control assay; error bars indicate standard errors; bars with different letters or symbols indicate significant differences ($p < 0.05$).
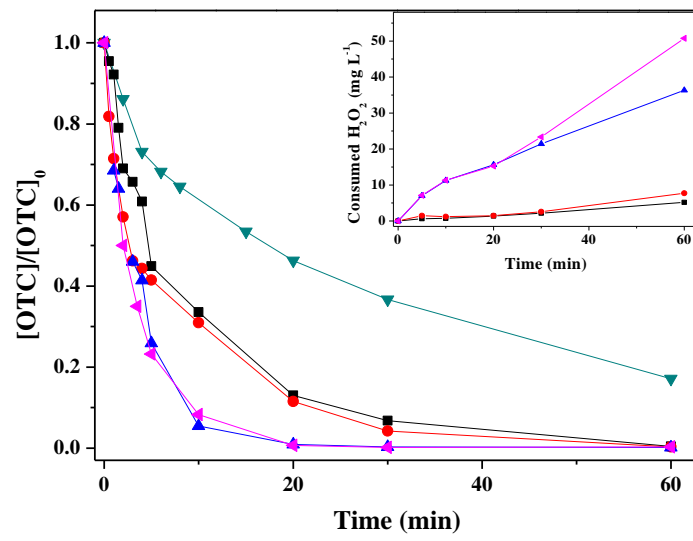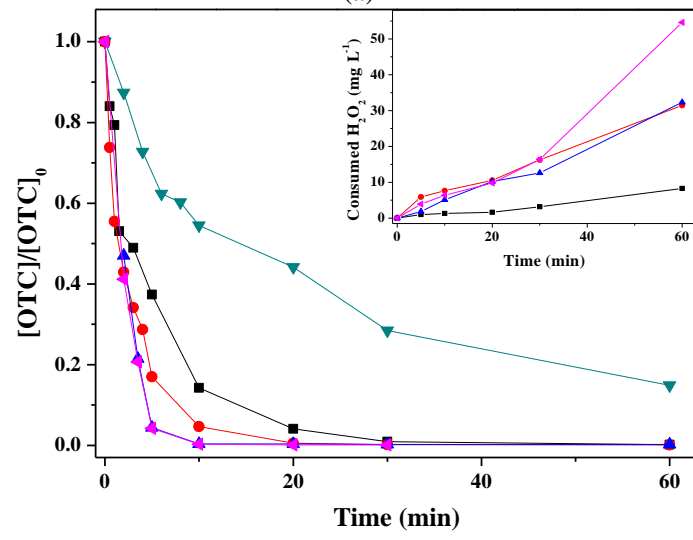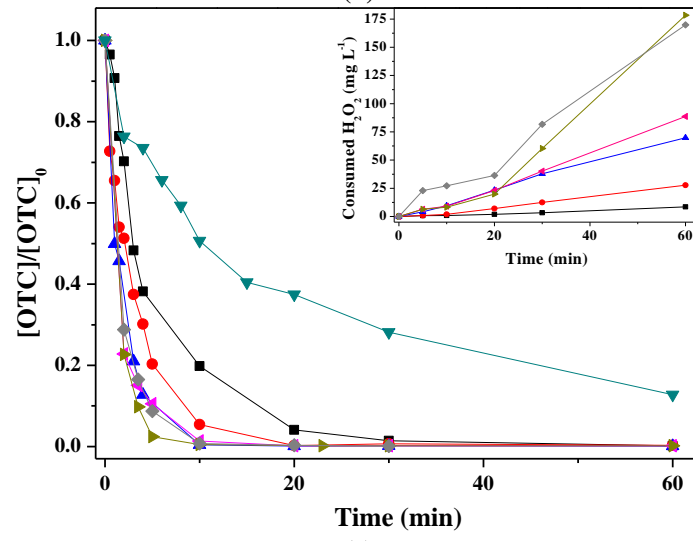
692

693

694   **Figure 1**
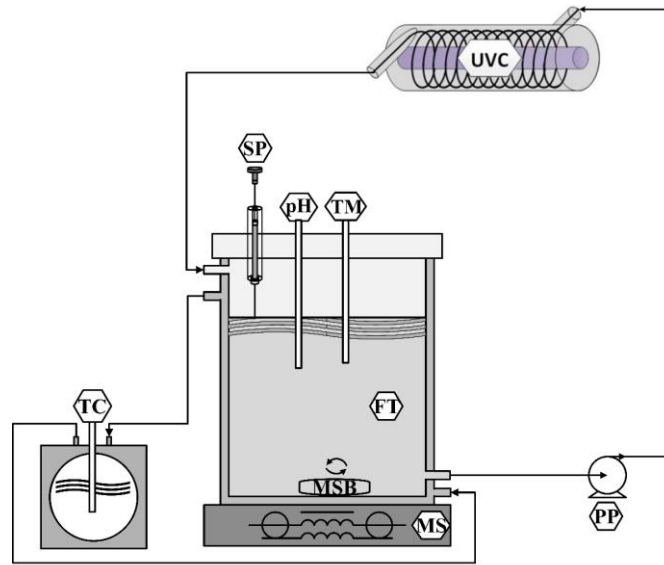
695

696
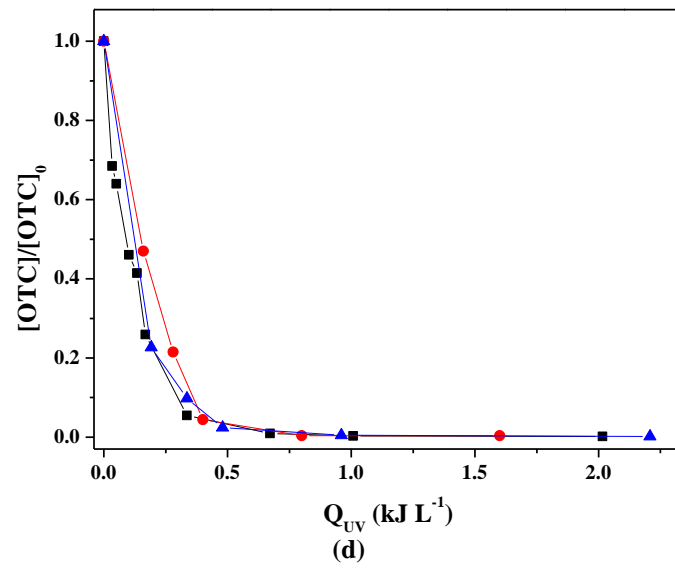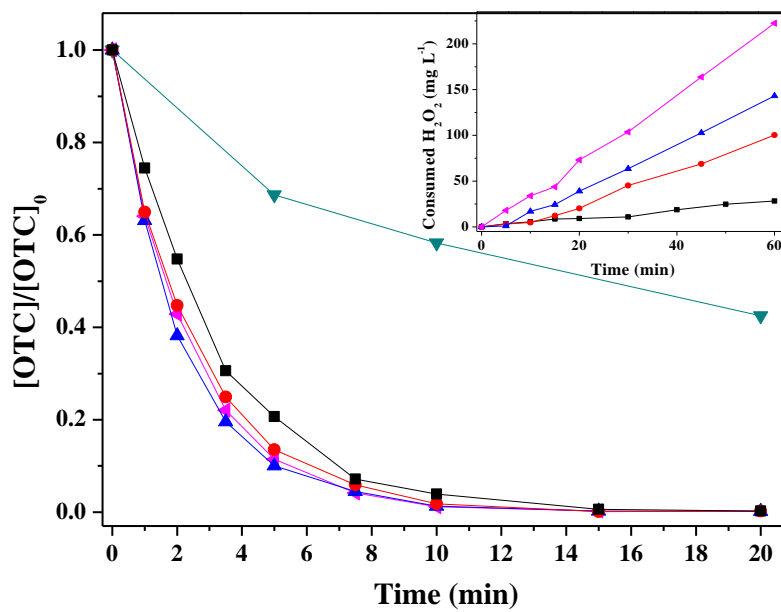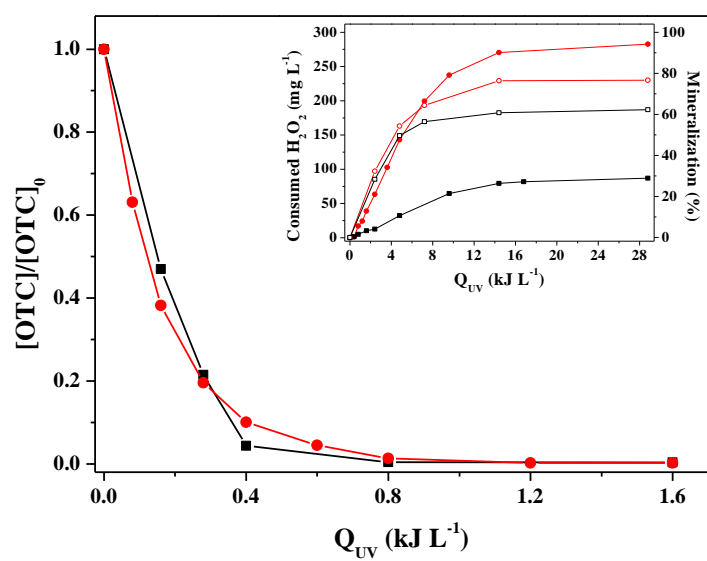
Figure 2

(a)

(b)

(c)

(d)

698

699

702
703

704

705

706

Figure 4

726   **Figure 5**

727

(a)
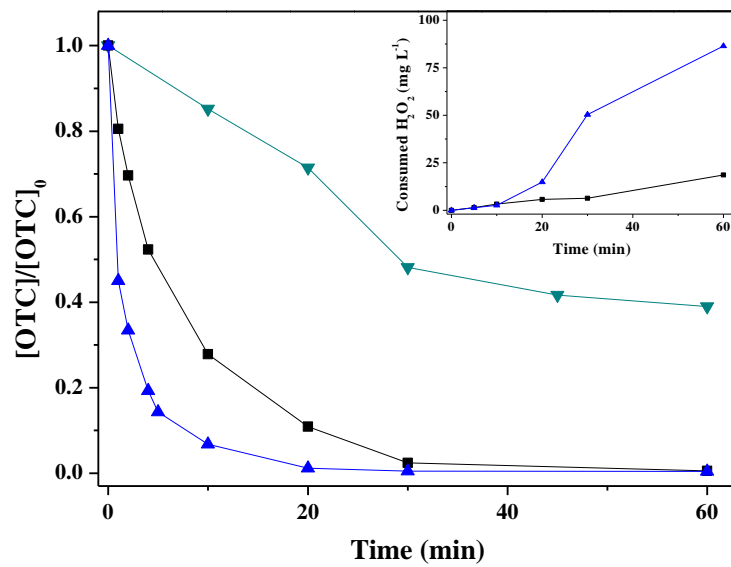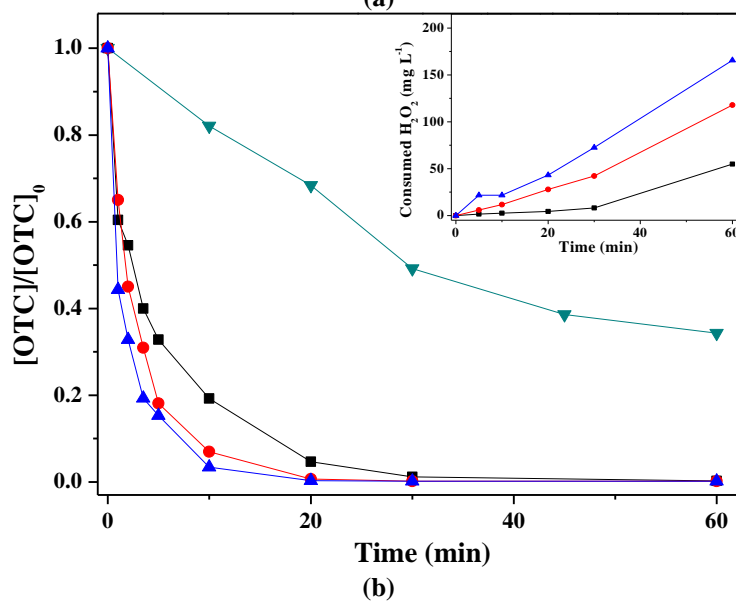
(b)

728

729

730 **Figure 6**

731

732

733 **Figure 7**

734
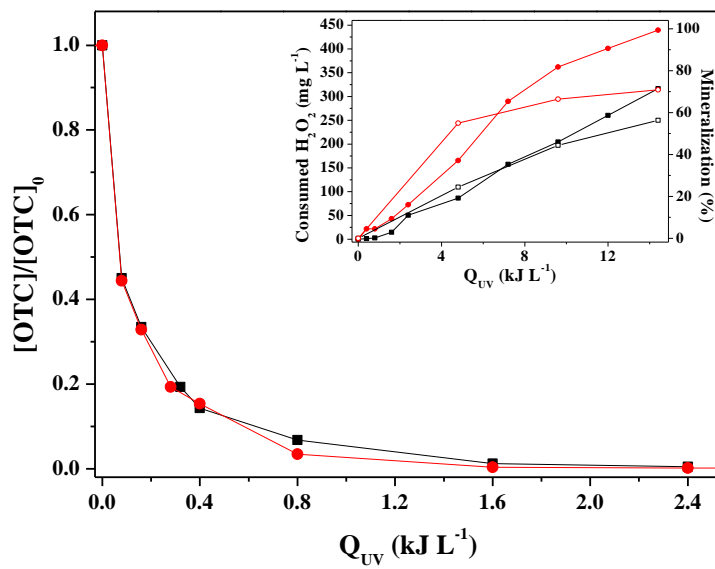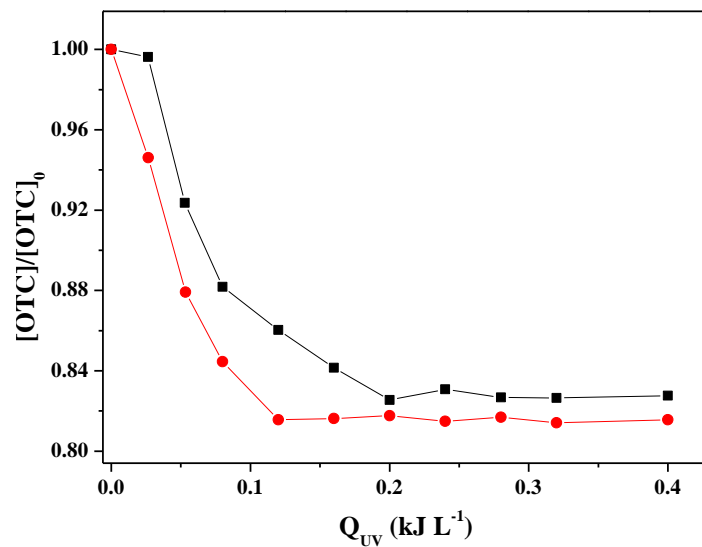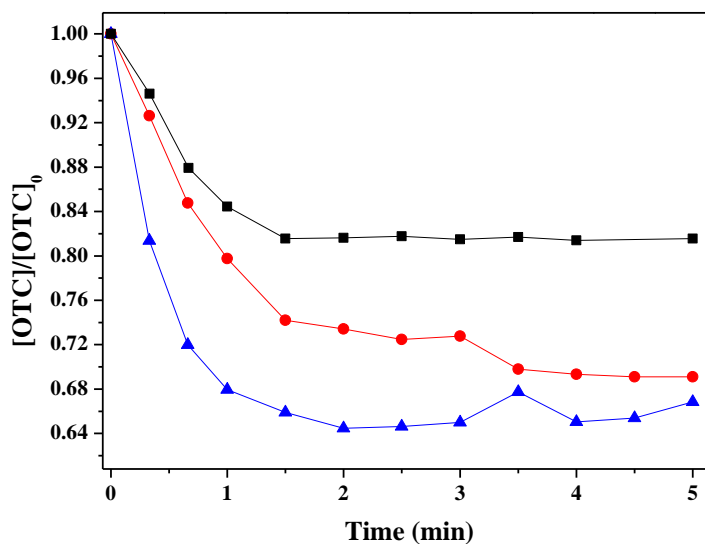

(a)

(b)

735

736

737

738

739

740

741

742

743 **Figure 8**
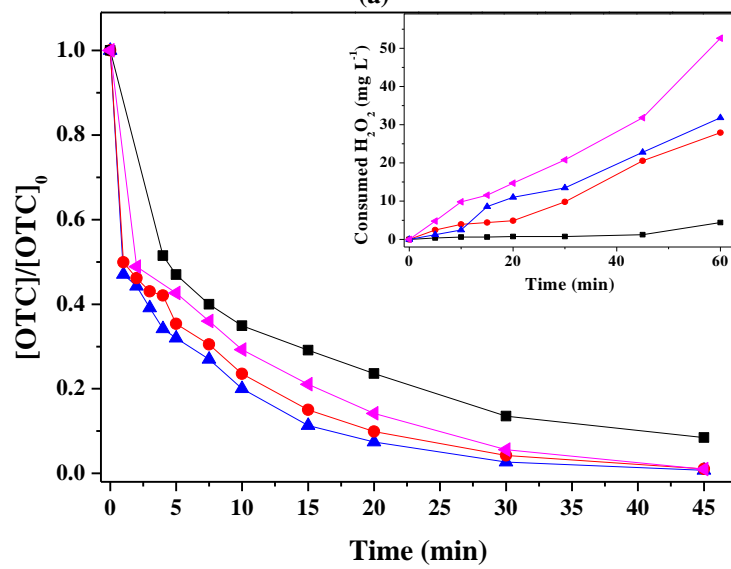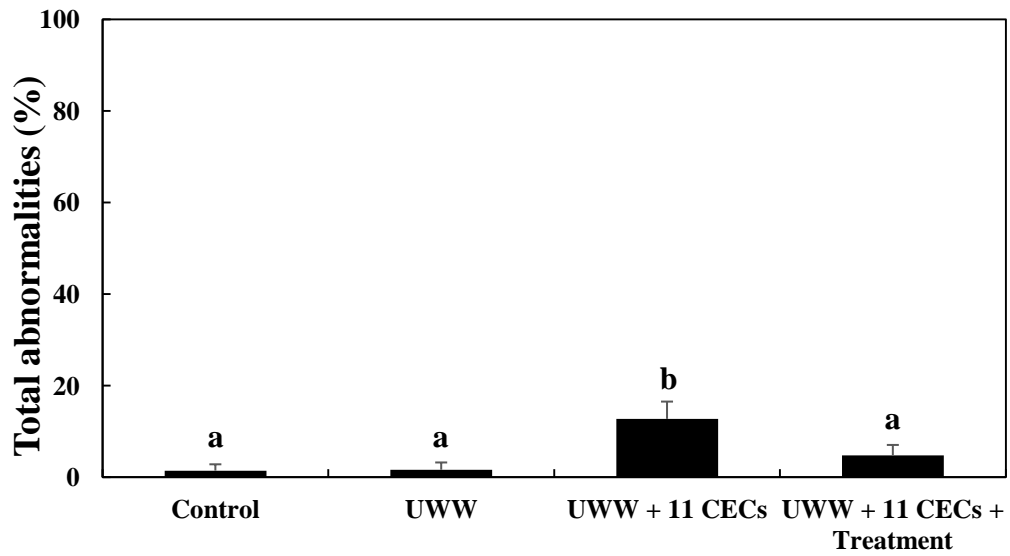

(a)
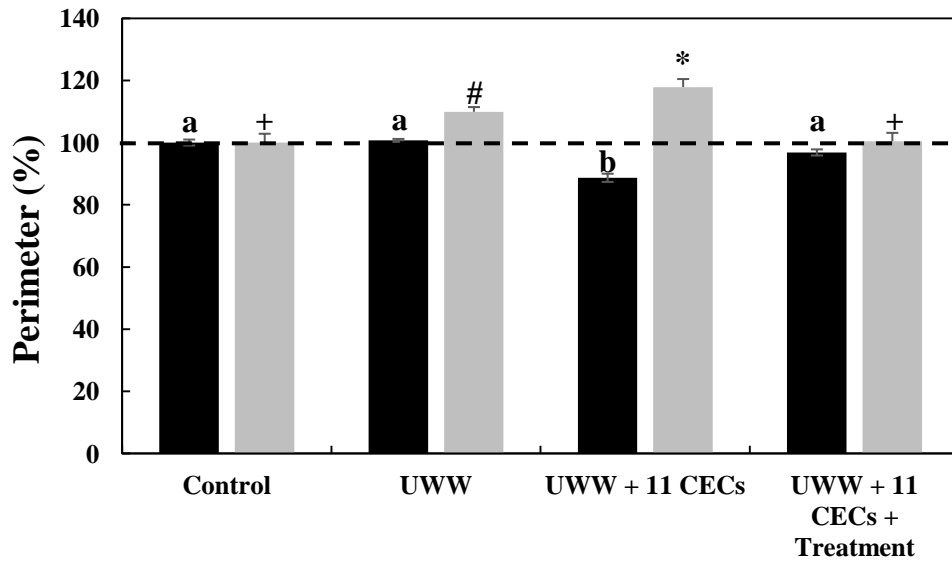

(b)

744

Figure 9

(a)

(b)
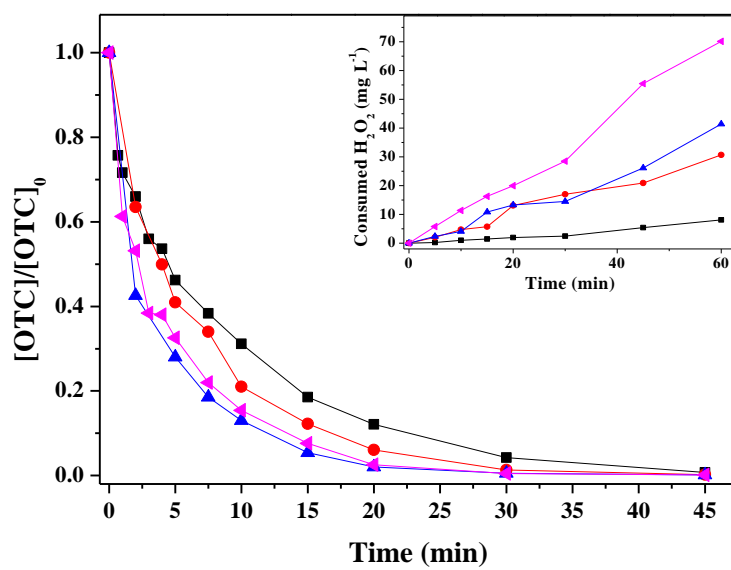
748   **Table 1.** Main physicochemical characteristics of the real urban wastewater collected
749   after secondary treatment.

Parameter (units)	Values
Color	Pale/Yellow
Odor	n.d.[a]
pH	6.5
Temperature (°C)	24.7
Turbidity (UNT)	1.0
Conductivity ($\mu S\ cm^{-1}$)	883
Dissolved oxygen (mg L^{-1})	3.8
Redox potential (mV)	-10
Total dissolved carbon (mg L^{-1})	51
Dissolved inorganic carbon (mg L^{-1})	33
Dissolved organic carbon (mg L^{-1})	18
Chemical oxygen demand (mg $O_2\ L^{-1}$)	56
Total dissolved iron (mg L^{-1})	0.26
Absorbance at 254 nm (AU)	0.21
Total suspended solids (mg L^{-1})	1.7
Volatile suspended solids (mg L^{-1})	1.7
Total dissolved nitrogen (mg L^{-1})	3.9
Total dissolved organic nitrogen (mg L^{-1})	2.7
Ammonium - $N-NH_4^+$ (mg L-1)	1.1
Nitrite - $N-NO_2^-$ (mg L^{-1})	<0.02
Nitrate - $N-NO_3^-$ (mg L^{-1})	0.09
Bromide - Br^- (mg L^{-1})	0.1
Chloride - Cl^- (mg L^{-1})	174
Phosphate - PO_4^{3-} (mg L^{-1})	12
Sulfate - SO_4^{2-} (mg L^{-1})	76
Calcium - Ca^{2+} (mg L^{-1})	57
Lithium - Li^+ (mg L^{-1})	<0.02
Magnesium - Mg^{2+} (mg L^{-1})	9.1
Potassium - K^+ (mg L^{-1})	29
Sodium Na^+ (mg L^{-1})	136
Total phosphorous - P (mg L^{-1})	4.8
Atenolol ($\mu g\ L^{-1}$)	1.1
Carbamazepine ($\mu g\ L^{-1}$)	4.8
Diclofenac ($\mu g\ L^{-1}$)	2.8
Metformin ($\mu g\ L^{-1}$)	2.1
Sulfamethoxazole ($\mu g\ L^{-1}$)	2.4
Trimethoprim ($\mu g\ L^{-1}$)	3.7

750   [a] n.d. - Not detected.

37

751   **Table 2.** Effect of H_2O_2 initial concentration in the removal of 11 pharmaceuticals spiked in a real urban wastewater by UVC/H_2O_2
752   photochemical system using a FluHelik photoreactor in multiple or single pass flow mode.

Name	Chemical Formula	Company	% Removal of ΣCECs in multiple pass flow mode (after 30 min)					% Removal of ΣCECs in single pass flow mode
			$[H_2O_2]_0$					
			10 mg L^{-1}	25 mg L^{-1}	50 mg L^{-1}	250 mg L^{-1}	500 mg L^{-1}	500 mg L^{-1}
Azytromicyn	$C_{38}H_{72}N_2O_{12}$	TCI	9.3	19	23	> 95	> 95	24
Naproxen	$C_{14}H_{14}O_3$	AlfaAesar	60	68	79	> 99	> 99	26
Atenolol	$C_{14}H_{22}N_2O_3$	AlfaAesar	27	42	62	> 99	> 99	35
Metformin	$NH_2C(=NH)NHC(=NH)N(CH_3)_2.HCl$	AlfaAesar	1.9	6.0	6.7	72	90	15
Bezafibrate	$C_{19}H_{20}ClNO_4$	AlfaAesar	40	51	66	> 99	> 99	18
Ibuprofen	$C_{13}H_{18}O_2$	AlfaAesar	30	38	63	> 99	> 99	35
Trimethoprim	$C_{14}H_{18}N_4O_3$	AlfaAesar	19	29	43	> 99	> 99	17
Carbamazepin	$C_{15}H_{12}N_2O$	ACROS organics	25	30	45	> 99	> 99	19
Sulfamethoxazole	$C_{10}H_{11}N_3O_3S$	TCI	98	99	> 99	> 99	> 99	25
Oxytetracycline	$C_{22}H_{24}N_2O_9.HCl$	AppliChem Panreac	92	96	98	> 99	> 99	32
Diclofenac	C14H10ClN.NaO2	Sigma Aldrich	96	98	97	> 99	> 99	31

753

Table 3. Pseudo-first order kinetic constants along with the corresponding coefficient of determination (R^2) and residual variance (S^2_r), photonic

efficiencies (ξ) and photochemical space time yields (PSTY) for degradation of 20 mg L⁻¹ of OTC at pH 7.5 and 25 ºC.

Experiment	$[OTC]_0$ (mg L⁻¹)	$[H_2O_2]$ (mg L⁻¹)	Q (L h⁻¹)	pH	$k \times 10^1$ (min⁻¹)	k (L kJ⁻¹)	R^2	S^2r (mg L⁻¹)²	$r_0 \times 10^2$ (mg L⁻¹ min⁻¹)	$\xi \times 10^2$	PSTY (m³_water m⁻³_reactor day⁻¹ kW⁻¹)
						Jets photoreactor - UVC lamp of 6 W					
1.1	5.1	0	100	4.5	0.17 ± 0.01	0.21 ± 0.01	0.989	0.02	0.018 ± 0.001	0.11	0.02
1.2	5.0	0	100	7.5[a]	0.30 ± 0.02	0.37 ± 0.03	0.963	0.08	0.032 ± 0.002	0.19	0.03
1.3	5.0	0	100	7.5	1.1 ± 0.1	1.4 ± 0.1	0.976	0.07	0.12 ± 0.01	0.70	0.12
						Jets photoreactor - UVC lamp of 4 W					
2.1	21.3	0	100	7.5	0.41 ± 0.04	1.2 ± 0.1	0.963	2.0	0.19 ± 0.02	2.6	0.10
2.2	20.9	20	100	7.5	1.3 ± 0.1	4.0 ± 0.3	0.976	1.3	0.6 ± 0.1	8.5	0.34
2.3	21.8	50	100	7.5	1.5 ± 0.2	4.6 ± 0.5	0.963	2.0	0.7 ± 0.1	10.3	0.40
2.4	19.9	100	100	7.5	2.7 ± 0.1	7.8 ± 0.4	0.988	0.6	1.2 ± 0.1	16.1	0.69
2.5	20.0	200	100	7.5	2.8 ± 0.1	8.2 ± 0.3	0.999	0.1	1.23 ± 0.04	17.2	0.73
						Jets photoreactor - UVC lamp of 6 W					
3.1	20.9	0	100	7.5	0.52 ± 0.05	0.65 ± 0.06	0.961	2.0	0.24 ± 0.02	1.4	0.06
3.2	22.0	20	100	7.5	2.4 ± 0.3	3.1 ± 0.3	0.968	2.1	1.2 ± 0.1	6.9	0.26
3.3	22.9	50	100	7.5	4.0 ± 0.3	5.0 ± 0.4	0.972	1.6	2.0 ± 0.2	11.7	0.43
3.4	20.2	100	100	7.5	5.0 ± 0.2	6.3 ± 0.2	0.998	0.1	2.2 ± 0.1	13.0	0.54
3.5	21.0	200	100	7.5	4.7 ± 0.2	5.9 ± 0.3	0.996	0.3	2.1 ± 0.1	12.6	0.51
3.6	20.8	100	50	7.5	2.2 ± 0.1	2.8 ± 0.2	0.992	0.5	1.0 ± 0.1	5.9	0.24
3.7	21.4	100	75	7.5	3.0 ± 0.3	3.7 ± 0.4	0.982	0.8	1.4 ± 0.1	8.2	0.32
						Jets photoreactor - UVC lamp of 11 W					
4.1	21.5	0	100	7.5	0.58 ± 0.04	0.61 ± 0.05	0.962	1.8	0.27 ± 0.02	1.3	0.05
4.2	21.0	20	100	7.5	2.0 ± 0.2	2.1 ± 0.2	0.983	1.2	0.9 ± 0.1	4.4	0.18
4.3	22.0	50	100	7.5	3.5 ± 0.2	3.6 ± 0.2	0.974	1.2	1.7 ± 0.1	8.2	0.32
4.4	21.3	100	100	7.5	5.18 ± 0.02	5.40 ± 0.02	0.999	0.1	2.40 ± 0.01	11.8	0.47
4.5	21.3	200	100	7.5	6.4 ± 0.1	7 ± 1	0.986	0.9	2.94 ± 0.03	14.4	0.57
4.6	20.6	500	100	7.5	7.2 ± 0.2	7.5 ± 0.2	0.999	0.1	3.2 ± 0.1	15.9	0.65
4.7	20.0	700	100	7.5	5.7 ± 0.3	5.9 ± 0.3	0.996	0.2	2.5 ± 0.1	12.1	0.51

FluHelik photoreactor - UVC lamp of 6 W											
5.1	22.1	0	100	7.5	0.5 ± 0.1	0.63 ± 0.06	0.983	1.21	0.24 ± 0.02	1.4	0.05
5.2	22.8	100	100	7.5	3.2 ± 0.1	4.0 ± 0.1	0.999	0.09	1.58 ± 0.03	9.3	0.35
5.3	22.2	200	100	7.5	4.0 ± 0.1	5.1 ± 0.1	0.999	0.04	1.95 ± 0.03	11.5	0.44
5.4	22.8	300	100	7.5	4.7 ± 0.1	5.8 ± 0.1	0.999	0.02	2.32 ± 0.03	13.7	0.50
5.5	22.6	400	100	7.5	4.32 ± 0.03	5.40 ± 0.04	0.999	0.01	2.12 ± 0.01	12.5	0.47
5.6	21.4	300	50	7.5	2.46 ± 0.03	3.08 ± 0.04	0.999	0.04	1.15 ± 0.02	6.8	0.27
5.7	21.3	300	75	7.5	4.0 ± 0.1	5.1 ± 0.1	0.999	0.06	1.87 ± 0.03	11.0	0.44
Real Urban Wastewater - Jets photoreactor - UVC lamp of 6 W											
6.1	19.8	0	100	7.5	0.16 ± 0.01	0.20 ± 0.01	0.996	0.19	0.07 ± 0.02	0.4	0.02
6.2	20.5	100	100	7.5	1.5 ± 0.1	1.9 ± 0.1	0.988	0.75	0.66 ± 0.05	3.9	0.16
6.3	20.9	500	100	7.5	4.6 ± 0.4	5.8 ± 0.5	0.986	0.78	2.1 ± 0.2	12.4	0.50
Real Urban Wastewater - FluHelik photoreactor - UVC lamp of 6 W											
7.1	20.3	0	100	7.5	0.2 ± 0.1	0.23 ± 0.01	0.976	0.97	0.08 ± 0.01	0.5	0.02
7.2	20.4	100	100	7.5	2.0 ± 0.1	2.5 ± 0.2	0.992	0.47	0.9 ± 0.1	5.1	0.21
7.3	20.1	300	100	7.5	3.3 ± 0.1	4.2 ± 0.1	0.998	0.09	1.45 ± 0.04	8.5	0.36
7.4	19.5	500	100	7.5	4.9 ± 0.4	6.1 ± 0.5	0.989	0.58	2.1 ± 0.2	12.1	0.53
7.5	19.9	500	50	7.5	4.0 ± 0.4	5.0 ± 0.4	0.981	0.98	1.7 ± 0.2	10.1	0.43
7.6	19.4	500	75	7.5	4.7 ± 0.4	5.8 ± 0.5	0.987	0.66	2.0 ± 0.2	11.6	0.50
Pilot-scale FluHelik photoreactor - UVC lamp of 95 W											
8.1	20.4	100	7500	7.5	1.3 ± 0.1	5.1 ± 0.3	0.983	0.69	0.58 ± 0.03	0.35	0.44
8.2	20.7	300	7500	7.5	1.6 ± 0.1	6.4 ± 0.4	0.982	0.78	0.74 ± 0.04	0.45	0.55
8.3	21.5	500	7500	7.5	2.5 ± 0.1	9.7 ± 0.1	0.999	0.01	1.18 ± 0.01	0.72	0.85
8.4	20.5	700	7500	7.5	2.3 ± 0.1	9 ± 1	0.980	0.80	1.0 ± 0.1	0.63	0.78
Real Urban Wastewater - Pilot-scale FluHelik photoreactor - UVC lamp of 95 W											
9.1	20.8	100	7500	7.5	0.8 ± 0.1	3.2 ± 0.2	0.978	0.93	0.37 ± 0.03	0.23	0.28
9.2	19.8	300	7500	7.5	1.5 ± 0.1	5.7 ± 0.3	0.995	0.22	0.63 ± 0.03	0.38	0.49
9.3	20.6	500	7500	7.5	1.7 ± 0.1	6.6 ± 0.4	0.983	0.66	0.8 ± 0.1	0.47	0.57
9.4	19.6	700	7500	7.5	1.3 ± 0.1	5.0 ± 0.4	0.974	0.98	0.55 ± 0.04	0.34	0.43

756 [a] without pH control

SUPPLEMENTARY MATERIAL

An Innovative Photoreactor, FluHelik, To Promote UVC/H₂O₂ Photochemical Reactions: Tertiary Treatment of an Urban Wastewater

Jonathan C. Espíndola[1,2], Raquel O. Cristóvão[1,*], Sara R.F. Araújo[1], Teresa Neuparth[3], Miguel M. Santos[3,4], Rosa Montes[5], José B. Quintana[5], Rosario Rodil[5], Rui A.R. Boaventura[1], Vítor J. P. Vilar[1,*]

[1]*Laboratory of Separation and Reaction Engineering - Laboratory of Catalysis and Materials (LSRE-LCM), Department of Chemical Engineering, Faculty of Engineering, University of Porto, Rua Dr. Roberto Frias, 4200-465, Porto, Portugal*

[2]*CNPq - National Council for Scientific and Technological Development, Brazil*

[3]*CIMAR/CIIMAR - LA, Interdisciplinary Centre of Marine and Environmental Research, Avenida General Norton de Matos S/N, 4450-208 Matosinhos, Portugal*

[4]*FCUP – Department of Biology, Faculty of Sciences, University of Porto, Rua do Campo Alegre, 4169-007 Porto, Portugal.*

[5]*Department of Analytical Chemistry, Nutrition and Food Sciences, IIAA—Institute for Food Analysis and Research, Universidade de Santiago de Compostela, Constantino Candeira S/N, 15782 Santiago de Compostela, Spain*

*Corresponding authors:

Raquel O. Cristóvão:
Tel: +351 22 041 3606; *E-mail*: raquel.cristovao@fe.up.pt
Vítor J. P. Vilar:
Tel: +351 91 825 7824; *E-mail:* vilar@fe.up.pt
Fax: +351 22 508 1674

OTC and LMWCA analytical determinations

OTC concentration was followed by HPLC using a VWR Hitachi ELITE LaChrom LC fitted with a Merck LiChrosorb® RP-18 (5 µm) LiChroCART® 125-4 column at 25 °C and a diode array detector (DAD). The equipment was operated in gradient mode using as mobile phase a mixture of acetonitrile/methanol/0.014M oxalic acid with ratios of 10:10:80 (v/v) from 0 to 3 min, 15:10:75 (v/v) from 3 to 5 min, 20:10:70 (v/v) from 5 to 7 min, and 10:10:80 (v/v) from 7 to 14 min. The flow rate was 0.8 mL min^{-1}. Samples of 50 µL were injected and the DAD was set at 354 nm. The retention time was 5.8 min and the limits of quantification and detection were 1.2 and 0.3 mg L^{-1} of OTC, respectively.

LMWCA concentrations were determined by ion-exclusion HPLC using the VWR Hitachi ELITE LaChrom LC fitted with a Phenomenex RezexTM ROA-Organic Acid H+ (8%) 300 mm × 7.8 mm column at room temperature (25 ºC). The mobile phase was 0.0025 M H$_2$SO$_4$ at a flow rate of 0.5 mL min^{-1}. Samples of 10 µL were injected and the DAD was set at 210 nm.

Table S1 - Instrumental LC-MS/MS parameters

Compound	Retention time (min)	Parent ion (m/z)	Fragment ion (m/z)	Cone voltage (V)	Collision energy (V)	ESI mode	LOQ ng mL^{-1}
Metformin	1.3	130	60	30	15	Pos.	0.04
		130	71	30	20		
Carbamazepine	8.3	237	194	20	25	Pos.	0.01
		237	179	20	40		
Sulfamethoxazole	6.4	254	92	30	25	Pos.	0.01
		254	156	30	15		
Atenolol	5.1	267	145	40	25	Pos.	0.02
		267	190	40	20		
Trimethoprim	6.2	291	123	40	30	Pos.	0.02
		291	230	40	30		
Oxytetracycline	6.7	461	426	40	20	Pos.	0.01
		461	443	40	10		
Azytromicyn	7.5	749.5	116	70	40	Pos.	1.8
		749.5	591	70	25		
Ibuprofen	9.4	205	161	20	5	Neg.	0.1
		205	159	20	5		
Naproxen	8.4	229	170	20	15	Neg.	0.04
		229	185	20	10		
Diclofenac	9.1	294	250	33	10	Neg.	0.1
		294	252	33	10		
Bezafibrate	8.5	360	274	33	15	Neg.	0.01
		360	154	33	30		

Ionization was performed in positive mode using the following parameters: 3.5 and 1.5 kV (capillary voltage in positive and negative modes, respectively), 150°C (source temperature), 350°C (desolvation temperature), 650 L/h (desolvation gas-N^2 flow) and 10 L/h (cone gas- N^2 flow). Collision energy (CE) and cone voltage (CV) values were adjusted individually for every transition (parent/fragment pair). For every compound the transitions selected for quantification are shown in the upper row and the qualifier transitions are shown in the lower row.
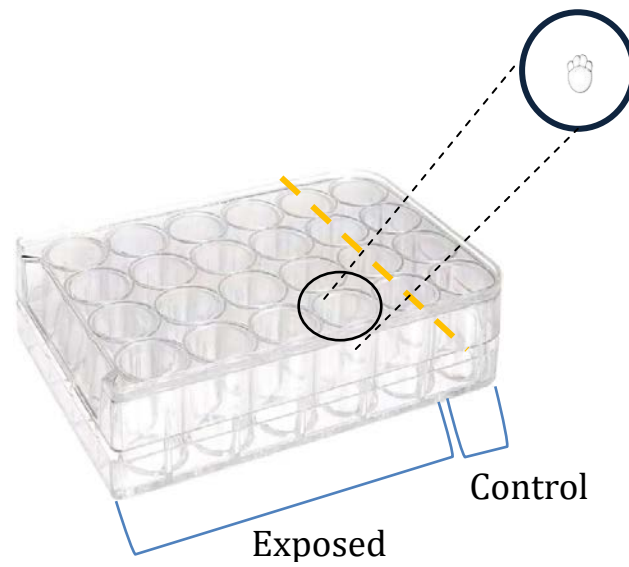
Figure S1 - Schematic representation of the experimental setup. In each 24-well plate was allocated one treatment (20 embryos; 1 embryo per well) plus an internal plate control (4 embryos). All the 24-well plates were maintained on a water bath at 26.5 ± 0.5 °C for 80 h.
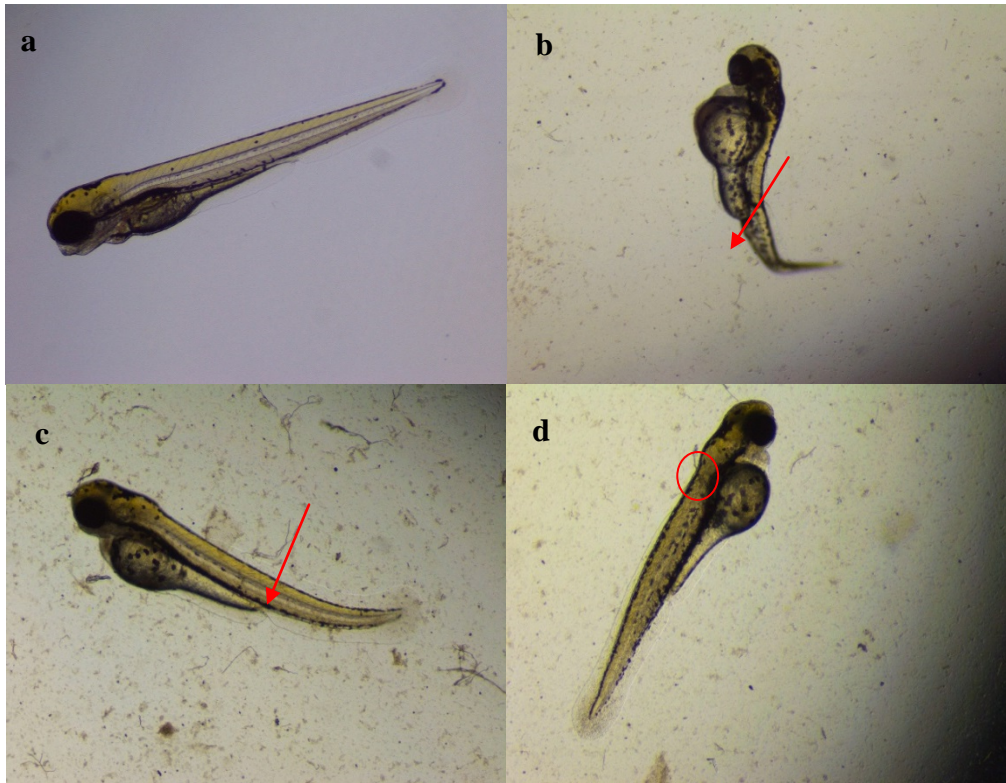
Figure S2 - Examples of different abnormalities detected in zebrafish embryos at 80 h: (a) normal embryo; (b) tail abnormality; (c) lordosis; (d) pericardial oedema.